



Universiteit
Leiden

The Netherlands

Soil organic amendments for climate-smart agriculture

Kok, D.D.

Citation

Kok, D. D. (2024, September 26). *Soil organic amendments for climate-smart agriculture*. Retrieved from <https://hdl.handle.net/1887/4093453>

Version: Publisher's Version

License: [Licence agreement concerning inclusion of doctoral thesis in the Institutional Repository of the University of Leiden](#)

Downloaded from: <https://hdl.handle.net/1887/4093453>

Note: To cite this publication please use the final published version (if applicable).

CHAPTER 2

Relationships of Priming Effects with Organic Amendment Composition and Soil Microbial Properties

Dirk-Jan Kok
Laura Scherer
Wim de Vries
Krijn Trimbos
Peter van Bodegom

Published in *Geoderma*; 422, 115951 (2022)
DOI: 0.1016/j.geoderma.2022.115951

ABSTRACT

Soil organic carbon (SOC) sequestration through the application of organic amendments (OAs) is considered an important strategy to offset anthropogenic CO₂ emissions while simultaneously enhancing soil quality and food security. The efficiency of SOC sequestration, however, depends on the priming effect which is influenced by interactions of OA composition with soil microbial response variables (MRVs). Yet, there remain large uncertainties surrounding the mechanisms and relationships defining these interactions, hampering the identification of OAs most effective for SOC sequestration and hindering the inclusion of OA dynamics in soil carbon models. In this study therefore, we performed an integrated assessment of these interactions for a cropland soil amended with wood chips, waterway residues, and isotopically enriched road-verge grasses, compost, and bokashi. Changes in 11 microbial properties and priming effects (for isotopically labelled OAs) were monitored for 150 days and related to 22 characterizations of OA composition. We demonstrate that i) hot water extractable to total carbon ratios of OAs are superior predictors of priming effects, ii) dissolvable to hot-water extractable carbon ratios are most closely related to variation in MRV expressions, and iii) priming effects correlate significantly with changes in several MRVs. Findings advocate for the adoption of energetic principles in modelling and predicting microbially-mediated soil carbon dynamics and suggest that application of OAs with high hot water to total carbon concentrations – potentially achievable by composting, but not fermenting, OAs prior to application – can allow for more efficient SOC sequestration.

Data in this chapter has been made publicly accessible in the DANS-Easy data repository under 10.17026/dans-xpp-dk4c.

Keywords: *Soil organic matter, carbon use efficiency, priming effect, carbon sequestration, soil microbial community*

2.1 INTRODUCTION

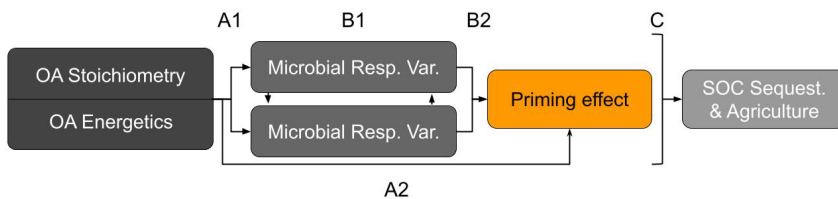
Over the past decades, unsustainable cultivation practices, such as intensive tillage, monocultures and crop residue removal, have significantly dwindled SOC stocks on arable land (Lal 2013). This reduction in SOC negatively affects soil quality as SOC is important for water retention, nutrient supply (Vogel et al. 2018) and soil structure (Lal 2013; Schlatter et al. 2017). The release of SOC as carbon dioxide (CO₂) furthermore increases greenhouse gas concentrations in the atmosphere, thus contributing to climate change. The overall importance of SOC sequestration for food security and climate change mitigation has been highlighted at the COP 21 in France in 2015, where the ‘4 per mille Soils for Food Security and Climate’ initiative was launched by the French Ministry of Agriculture (<http://4p1000.org/>). While there are uncertainties regarding the global potential of SOC sequestration, given concerns regarding associated nitrogen requirements (van Groenigen et al. 2017; de Vries 2018), it is estimated that worldwide application of best management practices could still sequester approximately 0.28 to 0.43 Gt C yr⁻¹ (Lessmann et al. 2021) – around 10% of the annual CO₂ flux.

Principles of climate-smart agriculture encourage soil management practices that promote SOC sequestration instead of SOC release. A primary means to sequester SOC involves increasing soil carbon inputs through the application of OAs such as green manure, livestock manure, and crop residues (Six et al. 2006; van der Wal and de Boer 2017). Analyses show, however, that the impact of OAs on soil carbon dynamics is strongly influenced by its interaction with the soil microbial community (Allison et al. 2013; Baldock et al. 2020; Kögel-Knabner 2017; Luo et al. 2018; Manzoni et al. 2010; Minasny and McBratney 2018; Wieder et al. 2013). Soil microorganisms can inhibit SOC sequestration by accelerating the decomposition of stable soil endogenous carbon – a phenomenon coined the priming effect (Blagodatskaya and Kuzyakov 2008; Guenet et al. 2018; Kuzyakov and Domanski 2000).

While important dynamics relating to the priming effect have been explored empirically and conceptually over the past decades, integral assessments presenting formalized, quantified relationships of priming effects with the agriculturally relevant OAs and changes in MRVs remain scarce (H. Wang et al. 2015). Some recent studies have made important contributions by identifying the existence of such relationships, revealing how priming is influenced by microbial biomass and soil nitrogen availability (Li et al., 2018), OA stoichiometry (Lijun Chen et al. 2019; Liu et al. 2020), rate of OA application (Liu et al. 2020), bacterial and fungal diversity (Lijun Chen et al. 2019), soil type and temperature (Fang, Singh, and Singh 2015), and more. Yet, the investigation of these relationships based on either limited diversity in OAs, a sparse number MRVs, use of artificial amendments

instead of natural ones, and/or a lack of quantification and comparison of observed relationships with different characterisations of OA composition leave major uncertainties regarding the OAs and OA properties most effective for SOC sequestration (Clocchiatti et al. 2020; Fang et al. 2020; Marzi et al. 2020; Stark et al. 2007). Such quantifications require the application of multiple, isotopically-labelled OAs of sufficient compositional diversity, as well as a sufficiently intensive sampling plan to cover the high temporal variability of the many different, relevant MRVs. Providing such an assessment would contribute to a greater and more informed utilization of OAs, thereby stimulating and improving the efficiency of SOC sequestration efforts.

In this research, we aim to improve our understanding of the relationships between different characterizations of OA composition, changes in MRVs and priming effects such that we may better predict and understand the mechanisms driving priming effects and the fate of carbon in the soil, particularly for natural OAs (Figure 2.1). We thereby: assess the performance of different characterizations of OAs for predicting changes in MRVs (A1) and the priming effect (A2); explore potential interactions between different MRVs (B1) and the priming effect (B2); and evaluate the overall impact of OA treatments for SOC sequestration and climate-smart agriculture (C).



Figure

2.1 Exploration of the relationship between different characterizations of OA composition with changes in microbial properties and processes (A1) and priming effects (A2); relationships among microbial properties and processes (B1) and with the priming effect (B2); and system implications for SOC sequestration for climate-smart agriculture (C).

For this purpose, we stoichiometrically and energetically characterized wood chips, waterway residues, as well as isotopically labelled unprocessed, composted and Bokashi fermented road-verge grasses and applied them to an agricultural Podzol soil. Subsequently, changes in microbial community size, structure, carbon respiration and nitrogen mineralization activity, and metabolic quotients were monitored over 150 days, while for the labelled OAs, we additionally calculated changes in CUE and priming effects. Relationships between different characterizations of OA composition with intermittent as well as peak changes in MRVs and priming effects, as well as among MRVs and priming effects, were identified through Pearson correlation analysis. The strongest linear relationships were subsequently evaluated in a regression analysis.

2.2 MATERIALS AND METHODS

2.2.1 Soil and amendments

Incubation (pot) experiments were performed on Podzol soil (WRB-FAO classification) acquired from an agricultural site in Haarlo, the Netherlands (52.10 N, 6.59 E). The soil was sieved at 2 cm and thoroughly homogenized before 50-gram dry weight equivalent (d.w.e.) aliquots were filled into sterile, polypropylene incubation pots. Samples were gravimetrically adjusted to and maintained at 60% water holding capacity with deionized water before being subjected to a fifteen-day preincubation period at 20°C prior to the start of the experiment.

The soil was amended with five OAs, which were selected based on the diversity in their composition and their local availability for agricultural application: i) wood chips, ii) reeds and weeds from waterways, iii) unprocessed road verge grasses, iv) composted road verge grasses, and v) Bokashi-fermented road verge grasses. The latter three treatments were isotopically enriched with ^{13}C to distinguish the exogenous organic matter derived from the (enriched) OA from the endogenous organic matter already present in the soil (natural abundance) after their application. This separation allowed us to determine the priming effect and CUE of different OA treatments. Non-labelled wood chips and reeds and weeds from waterways were included in the experiment to improve statistical power when evaluating changes in community size and composition, mineralization activity and metabolic quotients.

Woodchips were collected from a State Forestry Service collection point for woodchips produced from fallen tree branches (predominantly *Quercus Robur*) in the national park the Veluwe-Zoom (52.03 N, 6.05 E). Sun-dried reeds and weeds from waterways were recovered from the banks of a 5m-wide waterway in Zevenaar (51.94 N, 6.09 E). For road verge grasses, including compost and a Bokashi fermented product of those grasses, four plots of 25 cm² were excavated along a provincial motorway near Ede (52.04 N, 5.74 E). The grasses within each plot were trimmed to 1 to 2 cm and allowed to regrow over three months in climate-controlled growing chambers programmed to 70% relative humidity, 20°C ambient temperature, and a 12-hour light-dark cycle. Over the duration of the grass's recovery, the plots were biweekly pulse labelled with ^{13}C -CO₂ for carbon enrichment. The harvest was split into three fractions: i) unprocessed road verge grasses, ii) composted grasses, and iii) bokashi fermented grasses. For compost, one of the fractions of the grass harvest was inoculated with 10 ml of household compost leachate and subsequently matured in a perforated, high-density polyethylene container at 20 to 35°C. The compost was turned and regularly watered with tap water for six weeks before refrigerated storage at 4°C. For the Bokashi fermented product, another fraction of grasses was inoculated with a commercial Bokashi starter (EM®), moistened with demineralized water, placed upon a

plastic grill in an air-tight fermentation bucket and fermented for four weeks at 20 to 35°C. The Bokashi product was stored in an air-tight container at 4°C until the start of the experiment. Woodchips, waterway residues and the road verge grasses were air-dried and stored in paper bags.

All OAs were cut to a maximum size of 2 cm on the day of the start of the experiment. The experiment was performed in triplicate (n=3). For each treatment, 0.5 g d.w. of the organic amendment was manually mixed into 50 g of soil (1%, 0.01 g OA g⁻¹ soil) per replicate pot. Unamended control pots were also mixed to ensure equal disturbance across samples. Treatment pots were destructively sampled on days 3, 7, 16, 30, 60 and 150.

2.2.2 Amendment characterization

Organic amendments were characterized by their total (TOT), insoluble (IS), acid-hydrolysable (AH), hot-water soluble (HW) and dissolvable (DO) carbon and nitrogen fractions. These fractions are approximately representative of different biochemical fractions (e.g. cellulosic, ligneous, phenols and carbohydrates) and can be separated by stepwise, wet-chemical extractions (Ghani et al., 2003; Jones and Willett, 2006; Poeplau et al., 2018; Zhang et al., 2019). The OA total carbon and nitrogen (TOT: C_{TOT}, N_{TOT}, C_{TOT}:N_{TOT}) contents were determined from a dehydrated, ball-milled aliquot of OA by means of EA-IRMS. For the dissolvable fraction (DO: C_{DO}, N_{DO}, C_{DO}:N_{DO}), 0.5 g d.w. of OA was extracted with 45 ml of 0.05M potassium sulphate (K₂SO₄) for 1 h at room temperature on a vortex shaker. The hot-water soluble fraction (HW: C_{HW}, N_{HW}, C_{HW}:N_{HW}) was extracted from the residue of the K₂SO₄ extraction with 45 ml of 80°C deionized water for 18 hours. Both the DO and HW soluble extracts were separated from the residue by centrifugation for 10 minutes at 3000 rpm. The supernatant was recovered and centrifuged a second time for 10 minutes, filtered at 2.5 µm porosity using cellulose syringe filters, and dehydrated in a ventilated oven at 70°. The insoluble fraction (IS: C_{IS}, N_{IS}, C_{IS}:N_{IS}) was extracted through a two-step hydrolysis of a mixed sample of 200 mg OA and 300 mg pre-acid washed silicon sand. In the first hydrolysis step, the sample was mixed with 2 ml of 26N sulfuric acid (H₂SO₄) and shaken for 17 hours at room temperature. In the second hydrolysis step, the mixture was diluted to 2N and left to further hydrolyze at 90°C for 3 hours. The hydrolyzed sample was then centrifuged, supernatant discarded, washed thrice with demineralized water, and oven-dried at 70°C. DO and HW extracts, as well as IS residues, were weighed and shipped for analysis by EA-IRMS. The acid-hydrolysable fraction (AH: C_{AH}, N_{AH}, C_{AH}:N_{AH}) was calculated from the results of the elemental analysis as: AH = TOT – IS. Stoichiometric characterizations were based on the ratio of carbon to nitrogen concentrations in the different fractions. While recognizing that phosphorus can be an important component of an OA's stoichiometry (Cleveland and Liptzin, 2007; Heuck et

al., 2015), we decided to exclude it from our characterization given its limited inclusion in most soil carbon models. An overview of amendment characterization results is presented in

Table 2.1.

Table 2.1 Results of the stoichiometric and energetic characterization of OAs.

Amendment Characterization			Wood Chips	Waterway Resid.	Raw Grasses	Compost Grasses	Bokashi Grasses
Stoichiometric	C:N	C _{TOT} : N _{TOT} [mg mg ⁻¹]	57±3	11.5±0.4	11.4±0.7	10.1±0.2	13.3±0.7
		C _{IS} :N _{IS} [mg mg ⁻¹]	65.1±8.3	14±0.8	11.1±0.9	13.8±1.9	16.8±0.3
		C _{AH} :N _{AH} [mg mg ⁻¹]	45.8±11.5	9.4±0.8	12.7±5.7	4.9±1.4	7.8±1.5
		C _{HW} : N _{HW} [mg mg ⁻¹]	37.9±1.8	7.7±0.3	9±1.1	8.5±0.7	6.9±0.2
		C _{DO} : N _{DO} [mg mg ⁻¹]	11.7±0.8	5.7±0.4	7.9±0.7	8.7±0.6	9.7±0.6
Energetic	N	N _{TOT} [mg g ⁻¹]	8.3±0.4	33.2±0.8	32.4±1.5	25.1±0.4	28±1.2
		N _{IS} [mg g ⁻¹]	4.8±0.4	15.5±0.7	26.3±1.8	14.7±1.9	17.2±0.2
		N _{AH} [mg g ⁻¹]	3.5±0.6	17.7±1.1	6.1±2.3	10.4±2	10.9±1.2
		N _{HW} [mg g ⁻¹]	0.7±0	3.3±0.1	3.3±0.4	4±0.3	2.5±0
		N _{DO} [mg g ⁻¹]	0.4±0	2.2±0.1	5.4±0.2	2.9±0.2	1.9±0.1
	C	C _{TOT} [mg g ⁻¹]	474.6±6.6	382.6±8.4	370.4±14.5	254±3.8	373.2±12.4
		C _{IS} [mg g ⁻¹]	314.4±28.3	216.8±7.4	292.7±12.3	203.4±10	288.8±4.5
		C _{AH} [mg g ⁻¹]	160.2±29.1	165.8±11.2	77.7±19	50.5±10.7	84.4±13.2
		C _{HW} [mg g ⁻¹]	27.7±0.4	25.1±0.6	30.1±1.6	33.5±1.9	16.9±0.3
		C _{DO} [mg g ⁻¹]	4.6±0.3	12.4±0.9	42.9±3	25.3±0.7	18±0.7
C _x :C _{TOT}	C _{IS} : C _{TOT} [μg mg ⁻¹]	C _{IS} : C _{TOT} [μg mg ⁻¹]	662.5±60.3	566.7±23	790.2±45.3	801±41.1	773.8±28.3
		C _{AH} : C _{TOT} [μg mg ⁻¹]	337.5±61.4	433.3±30.8	209.8±51.9	199±42.2	226.2±36
		C _{HW} : C _{TOT} [μg mg ⁻¹]	58.4±5.3	65.6±2.7	81.1±4.7	131.8±6.8	45.3±1.7
		C _{DO} : C _{TOT} [μg mg ⁻¹]	9.6±0.6	32.3±2.4	115.7±9.4	99.4±3.1	48.2±2.4
C _{DO} :C _x	C _{DO} : C _{IS} [μg mg ⁻¹]	C _{DO} : C _{IS} [μg mg ⁻¹]	14.5±1.6	57±4.4	146.5±12.1	124.1±7	62.3±2.6
		C _{DO} : C _{AH} [μg mg ⁻¹]	28.6±5.5	74.6±7.2	551.5±140.3	499.7±106.6	213±34.2
		C _{DO} : C _{HW} [μg mg ⁻¹]	165.1±10.9	492.3±36.2	1426±126.2	754.2±47.9	1063±44.2

2.2.3 Microbial response variables

Five MRVs were measured, from which two expressions for priming effect and six other MRVs were derived. Total microbial biomass carbon concentration, bacterial and fungal DNA concentrations, mineralization activity as respired CO₂-C, and mineral nitrogen concentrations (NH₄⁺-N + NO₃-N + NO₂-N) were measured through wet-chemical extraction, droplet digital polymerase chain reaction (ddPCR), headspace sampling, and/or colourimetric methods as described in the sections below. Total (bacterial plus fungal)

microbial DNA concentrations, fungal to bacterial DNA ratios, cumulative carbon respiration, cumulative nitrogen mineralization, CUE, metabolic quotients (qCO_2), priming rates and cumulative priming were calculated, as described in section 2.4, based on measured MRVs.

2.2.3.1 Determination of microbial biomass carbon and microbial community composition

Microbial biomass carbon was determined based on the chloroform-fumigation technique (Brookes et al. 1985; Vance, Brookes, and Jenkinson 1987). In summary, 12.00 g of incubated soil per incubation sample was weighed into a small glass bowl. The bowls were placed within a vacuum-desiccator together with a beaker of 40 ml of ethanol-free chloroform ($CHCl_3$) and boiling chips. A thin film of demineralized water was added to the desiccator to maintain humidity during fumigation. A vacuum was drawn with a vacuum pump, and the chloroform was allowed to boil for 90 seconds before the valve connecting the desiccator to the vacuum pump was closed and the pump was switched off. Five hours after the initial boiling, the valve was reopened, a vacuum was drawn again, and the chloroform was allowed to boil a second time for 90 seconds, after which the valve was closed and the pump was switched off again. The samples were left under vacuum for precisely 24 hours in the dark at room temperature before the desiccator was reopened for an hour to allow any remaining $CHCl_3$ to dissipate. The fumigated samples were subsequently extracted with 45 ml of 0.05M potassium sulphate (K_2SO_4) on a vortex shaker for one hour. Extracts were dried and sent for analysis by EA-IRMS. The difference in carbon concentration between the fumigated and non-fumigated samples is proportional to the total microbial biomass, which was calculated by multiplying the difference in concentration between the fumigated and non-fumigated samples with an extraction-lysing efficiency factor $K_{EC}=0.38$ (Joergensen 1996). Results were corrected for soil gravimetric water content.

Microbial fungal to bacteria ratios (F:B) provide a functional and easily interpretable indicator for microbial community composition, resulting in their frequent quantification in soil ecological studies focusing on land and nutrient management (Malik et al. 2016). Here, we determined F:B based on fungal and bacterial DNA concentrations quantified through droplet digital PCR (ddPCR). ddPCR has been shown to be an accurate and sensitive tool for the absolute quantification of DNA (Doi et al. 2015:2; Hindson et al. 2013; Nathan et al. 2014). Unlike the conventional quantitative PCR (qPCR), ddPCR has a higher reproducibility, is generally less sensitive to inhibitors, and does not require calibration curves or high replicate counts (Doi et al. 2015; Hindson et al. 2013; Nathan et al. 2014; Yang et al. 2014). The protocol for quantification of F:B ratio by ddPCR is inspired by work from Trimbos et al.(2021) and is described in Appendix A. In addition to the ratio of

fungal to bacterial DNA concentrations, the sum of both DNA concentrations was taken as a second indicator for total microbial abundance.

2.2.3.2 Determination of carbon and nitrogen mineralization activity

Carbon respiration was determined by headspace sampling. Twenty-four hours prior to chemical extraction, the incubated soil samples were sealed in 500-ml septa jars and stored in a dark, 20°C incubator. Headspace samples were collected using a 10-ml glass, stopcock, gas syringe. A volume of 6 ml was withdrawn from the headspace of each jar and injected into a 5.9 ml flat-bottom evacuated exetainer. The exetainers were stored in the dark at room temperature until analysed for CO₂ concentration and δ¹³C signature using a gas chromatograph (Thermo Finnigan Trace) coupled to an IRMS (Thermo Scientific Delta 5) at Wageningen University & Research.

Mineral nitrogen was extracted with 1M potassium chloride (KCl) at ratios of 25 ml per 14.00 g of soil. Ammonium (NH₄⁺) and nitrate+nitrite (NO₃⁻+NO₂⁻) concentrations in each extract were determined colourimetrically in a procedure outlined by Sattolo et al. (2016) based on work by Mulvaney (1996) and Miranda et al. (2001) (Appendix B). Subsequently, the total mineral nitrogen content (N_{min}) was calculated as the sum of nitrogen in ammonium (NH₄⁺-N) and combined nitrate-nitrite fractions (NO₂⁻-N +NO₃⁻-N).

2.2.4 Calculations

2.2.4.1 Organic amendment and soil-derived carbon fractions

To determine CUE and priming effects, the isotopically labelled, exogenous organic matter in OAs was distinguished from endogenous organic matter in the soil through isotope tracing. δ¹³C (‰) enrichment was expressed in reference to the international Vienna-Pee Dee Belemnite (VPDB) standard by eq. 2.1:

$$\delta^{13}\text{C} = [(R_{\text{sample}}/R_{\text{VPDB}}) - 1] \cdot 1000 \quad (2.1)$$

Where R_{sample} is the measured isotope ratio of the sample, and R_{VPDB} is the isotope ratio of the International Vienna-Peedee Belemnite standard ($R_{\text{VPDB}} = 0.0112372$). A two end-member mixing model was subsequently applied to separate the fraction of exogenous organic carbon from total organic carbon concentrations (eq. 2.2) (Amelung et al. 2008):

$$F_{OA} = \frac{at\%_{final} - at\%_{initial}}{at\%_{OA} - at\%_{initial}} \quad (2.2)$$

Where F_{OA} is the fraction of OA derived carbon; $at\%_{final}$ is the bulk measured ^{13}C isotope abundance; $at\%_{initial}$ is the original ^{13}C isotope abundance of the unamended soil, and $at\%_{OA}$ is the ^{13}C isotope abundance of the enriched OA. The concentration of OA-derived carbon was calculated by multiplying F_{OA} with the bulk carbon concentration of the pool or flux.

2.2.4.2 Carbon-use efficiency and metabolic quotient

The carbon-use efficiency (CUE; %) is defined as the ratio of carbon incorporated into biomass to the sum of carbon incorporated into biomass and respired as a CO_2 by-product, and is calculated following eq. 2.3 (Geyer et al., 2019):

$$CUE = \delta^{13}\text{MBC} / [\delta^{13}\text{MBC} + \delta^{13}\text{R}_C] \cdot 100 \quad (2.3)$$

Where $\delta^{13}\text{MBC}$ is the amount of OA derived-carbon incorporated into microbial biomass carbon (MBC: $\mu\text{gMBC} \cdot \delta^{13}\text{C g}^{-1}$) and $\delta^{13}\text{R}_C$ is the cumulative respired OA-derived CO_2 -carbon ($\mu\text{gCO}_2 \cdot \delta^{13}\text{C}$). $\delta^{13}\text{MBC}$ was calculated following eq. 2.4 and eq. 2.5 described by Geyer et al. (2019).

$$at\%_{\text{MBC}} = \frac{at\%_{\text{DOC}_F} \cdot \text{DOC}_F - at\%_{\text{DOC}_{NF}} \cdot \text{DOC}_{NF}}{(\text{DOC}_F - \text{DOC}_{NF})} \quad (2.4)$$

$$\delta^{13}\text{MBC} = (\text{DOC}_F - \text{DOC}_{NF}) \cdot \frac{at\%_{\text{MBC}_t} - at\%_{\text{MBC}_c}}{at\%_{\text{OA}} - at\%_{\text{MBC}_c}} \quad (2.5)$$

Where $at\%_{\text{DOC}_F}$, DOC_F , $at\%_{\text{DOC}_{NF}}$, and DOC_{NF} represent the atom % and total C concentrations ($\mu\text{g C g}^{-1}$ soil) of fumigated (F) and non-fumigated (NF) K_2SO_4 soil extracts, respectively; $at\%_{\text{MBC}_t}$ and $at\%_{\text{MBC}_c}$ are the atom % of sample treatments and natural abundance controls, and $at\%_{\text{OA}}$ is the atom % of the OA.

The microbial metabolic quotient ($\mu\text{g CO}_2\text{-C } \mu\text{g}^{-1} \text{MBC d}^{-1}$), which represents the microbial respiration per unit microbial biomass, was calculated as: $Q_{CO_2} = R/MBC$ where R represents the respiration rate ($\mu\text{gCO}_2\text{-C g}^{-1}\text{d}^{-1}$) and MBC ($\mu\text{g g}^{-1}$) the total microbial biomass carbon concentration.

2.2.4.3 Priming rate and cumulative priming

The priming rate ($\mu\text{gCO}_2\text{-C g}^{-1}\text{soil d}^{-1}$) represents the additionally respired carbon from the endogenous soil carbon pool after application of an OA. We calculated the priming rate by eq. 2.6:

$$\delta^{13}PR = R_{Soil}^{trt} - R_{Soil}^{control} \quad (2.6)$$

Where R_{Soil}^{trt} ($\mu\text{gCO}_2\text{-C g}^{-1}\text{d}^{-1}$) is the rate of soil-derived CO_2 respiration for a given OA treatment, and $R_{Soil}^{control}$ ($\mu\text{gCO}_2\text{-C g}^{-1}\text{d}^{-1}$) is the rate of soil-derived CO_2 respiration for the unamended, control soil. The R_{Soil}^{trt} is calculated following eq. 2.7:

$$R_{Soil}^{trt} = (1 - F_{R,OA}) \cdot R_{Total}^{trt} \quad (2.7)$$

Where $F_{R,OA}$ is the fraction of OA-derived CO_2 as calculated per eq. 2.2, and R_{Total}^{trt} ($\mu\text{gCO}_2\text{-C g}^{-1}\text{d}^{-1}$) is the total respiration rate (soil and OA derived) for a given OA treated soil. The cumulative primed carbon was calculated as the average priming rate between every two sampling intervals, multiplied by the time difference between those intervals, and then summed with the amounts of primed carbon calculated each preceding step.

2.2.5 Data analysis

To determine which OA components demonstrate the closest relationship to changes in MRVs and priming effects, Pearson correlation coefficients (R) were calculated per sampling day for each combination of OA components with MRVs or priming effects. OA components with a higher number of significant correlations ($p < 0.05$) across all sampling days were considered better predictors of specific soil responses than others. Subsequently, predictions of peak changes in MRVs and priming effects were quantified through linear regression of OA components that demonstrated the highest, significant correlation ($|R| > 0$, $p < 0.05$) with the maximum response of MRVs across all sampling days. The choice was made to quantify the peak response, as it is most indicative of different OA effects and most directly comparable across studies. Finally, the relationships between the most significantly correlated pairs of MRV were quantified through linear regression using data from all sampling days and all treatments.

2.3 RESULTS

2.3.1 Priming effect and carbon balances for isotopically labelled amendment treatments

150 days after OA application, soils treated with isotopically labelled OAs showed differences in priming effects, soil carbon stocks, and OA-derived respired carbon (Figure 2.2A) while showing approximately equal *total* carbon stocks, i.e. the sum of soil and OA stocks (Figure 2.2B). Treatments demonstrated minor differences in soil carbon stocks, with more soil carbon being retained in the compost amended soil than for the untreated grasses and bokashi amended soils due to a larger priming effect for the latter two. Despite the lower carbon concentration of the initially applied compost compared to the other OA treatments, all soils had approximately equal OA carbon stocks at the end of the experiment. This occurs because of the relatively greater mineralization of OA carbon in the grasses- and bokashi-amended soils, ultimately negating the effect of their greater initial OA carbon concentrations.

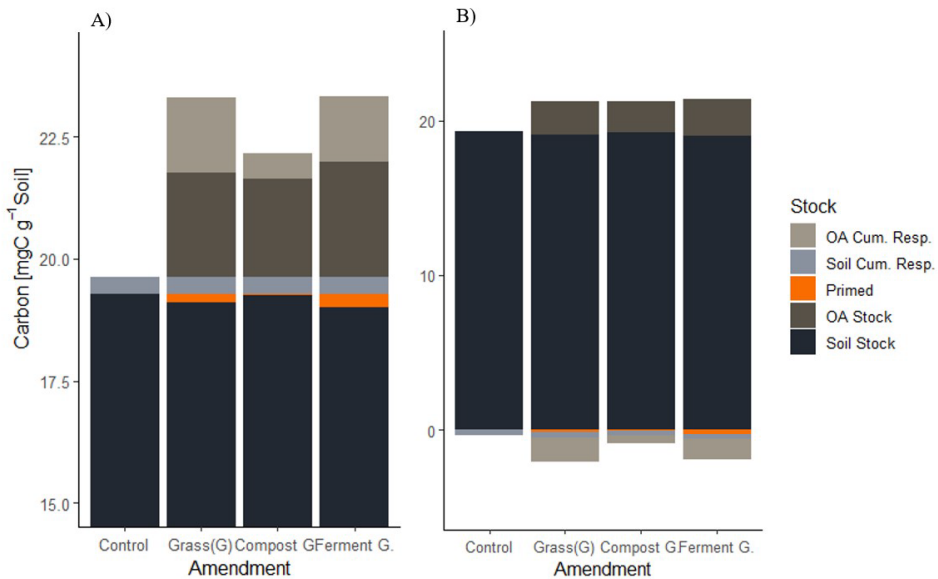


Figure 2.2 Carbon balances on day 150 for the unamended control soil and soils amended with isotopically labelled OAs; A) expressed as a combination of carbon stocks and fluxes to emphasize differences between treatments in priming effects and respiration rates, and B) as soil stocks on the positive y-axis and respiration fluxes on the negative y-axis to illustrate their relative sizes. Dark bars show mean carbon stocks in the soil and OA fractions, while lighter bars show the mean, cumulative carbon respired therefrom. The orange bars show the amount of carbon primed (i.e. additionally respired) from the soil pool due to OA application. Note also the interrupted y-axis for subplot A which begins at 15 mgC g⁻¹ Soil. n=3 for each bar.

2.3.2 Relationships between organic amendment composition and priming effect

Priming rates and cumulative priming, together denoted as priming effects, showed similar trends in time for unprocessed and (Bokashi) fermented grasses but not for composted grasses (Figure 2.3A,C). Priming rates for unprocessed and fermented grasses increased and peaked on the third day before steadily declining, whereas rates for the composted grasses decreased and showed a minimum within the first seven days before steadily increasing (Figure 2.3A). Cumulative priming was positive and increased continuously for unprocessed and fermented grasses across all days. For compost, it was negative and decreased in the first 59 days, after which it increased until day 150 (Figure 2.3C). By the end of the experiment, all treatments had approximately the same priming rate though still demonstrating large differences in cumulative priming. Cumulative priming and peak priming rates are similarly different between treatments, suggesting that final cumulative primed amount is largely influenced by the attained peak priming rate. Final cumulative priming and peak priming rate thus correlated similarly with different characterizations of OA composition, both demonstrating strongest linear correlations with the $C_{HW}:C_{TOT}$ ratio (Figure 2.3B, D, Table 2.2).

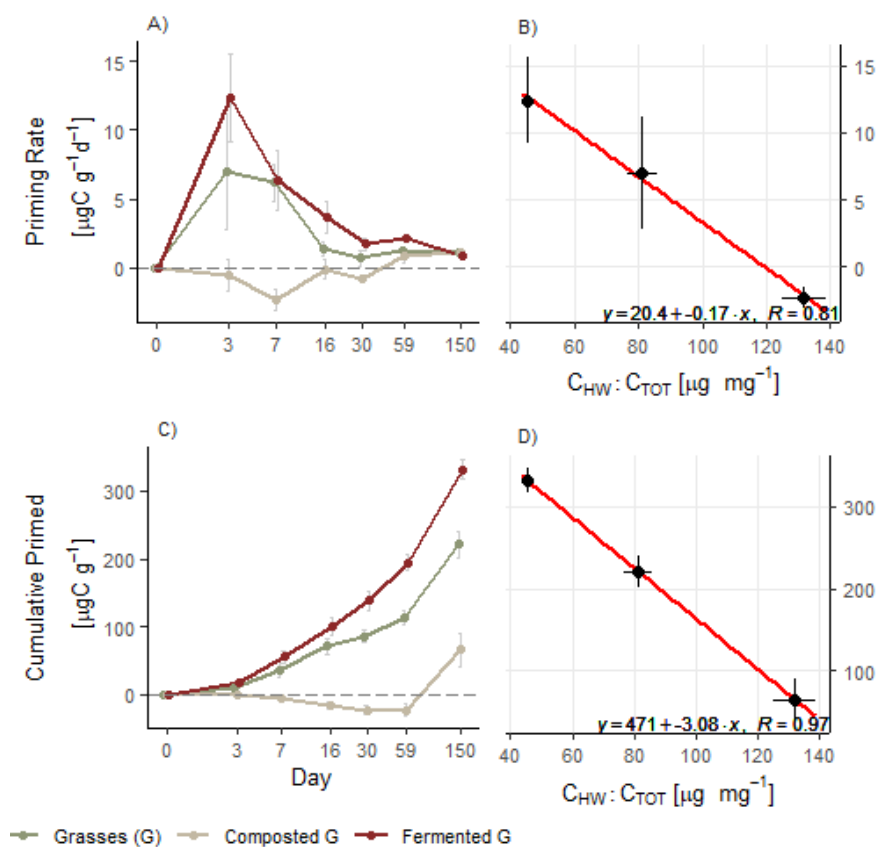


Figure 2.3 Temporal response and linear regression of peak response with highest correlative OA component for priming rates (A, B) and cumulative priming (C, D) for unprocessed, composted and bokashi-fermented road verge grasses. $n=3$ for each mean data point with standard error as error bars.

Table 2.2 Pearson correlation coefficients for peak priming rate and the cumulative priming for different OA components. The highest correlation coefficient per MRV is emboldened.

Component		Priming		
		Rate	Cumulative	
Stoichiometric	C:N	C _{TOT} : N _{TOT}	0.78*	0.95***
		C _{IS} :N _{IS}	0.31	0.42
		C _{AH} :N _{AH}	0.41	0.44
		C _{HW} : N _{HW}	-0.48	-0.62
		C _{DO} : N _{DO}	0.34	0.46
Energetic	N	N _{TOT}	0.44	0.47
		N _{IS}	0.28	0.29
		N _{AH}	-0.05	-0.01
		N _{HW}	-0.79*	-0.95***
		N _{DO}	-0.11	-0.18
	C	C _{TOT}	0.76*	0.89**
		C _{IS}	0.74*	0.86**
		C _{AH}	0.80**	0.94***
		C _{HW}	-0.72*	-0.88**
		C _{DO}	-0.11	-0.18
C _x :C _{TOT}	C _{IS} : C _{TOT}	-0.78*	-0.94***	
	C _{AH} : C _{TOT}	0.78*	0.94***	
	C _{HW} : C _{TOT}	-0.81**	-0.97***	
	C _{DO} : C _{TOT}	-0.5	-0.63	
C _{DO} :C _x	C _{DO} : C _{IS}	-0.48	-0.62	
	C _{DO} : C _{AH}	-0.55	-0.70*	
	C _{DO} : C _{HW}	0.48	0.53	

2.3.3 Relationships between priming effects and microbial response variables

Priming effects were also significantly correlated with several MRVs (Table 2.3). Most notably, priming rate correlated strongly with biomass carbon, microbial DNA-concentrations and qCO₂, while cumulative priming correlated strongly with CUE, nitrogen mineralization rates, and other cumulative properties.

Table 2.3 Pearson correlations for priming response with MRVs.

Correlations between Priming and MRVs	Priming Rate	Primed Carbon
Bacterial - DNA	0.69***	0.01
Fungal - DNA	0.38**	-0.03
F+B - DNA	0.69***	0
Biomass - CF.	0.73***	-0.09
F:B	0.2	0.04
CO ₂ - Rate	0.72***	-0.26
CO ₂ - Cum.	-0.09	0.88***
N _{min} - Rate	0.16	-0.31*
N _{min} - Cum	-0.16	0.56***
CUE	0.34*	-0.39**
qCO ₂	0.75***	-0.15

Not all linear correlations of priming effects with MRVs were equally convincing (Figure 2.4). While the linearity between priming rate and microbial DNA concentrations and carbon biomass is evidential (Figure 2.4A, B), the relationship of priming rate with CUE and qCO₂ appeared to largely be influenced by one to two extreme data points (Figure 2.4C, D). The relationship between cumulative priming and cumulative carbon respiration and nitrogen mineralization rates are convincingly linear but also not very insightful, as the relationship between accumulated variables is largely defined by the shared premise that they both increase over time (i.e. accumulate; Figure 2.4E, F). The nature of relationship between cumulative priming and CUE, furthermore, approaches more of an inverse-logarithmic trend than linear one (Figure 2.4G).

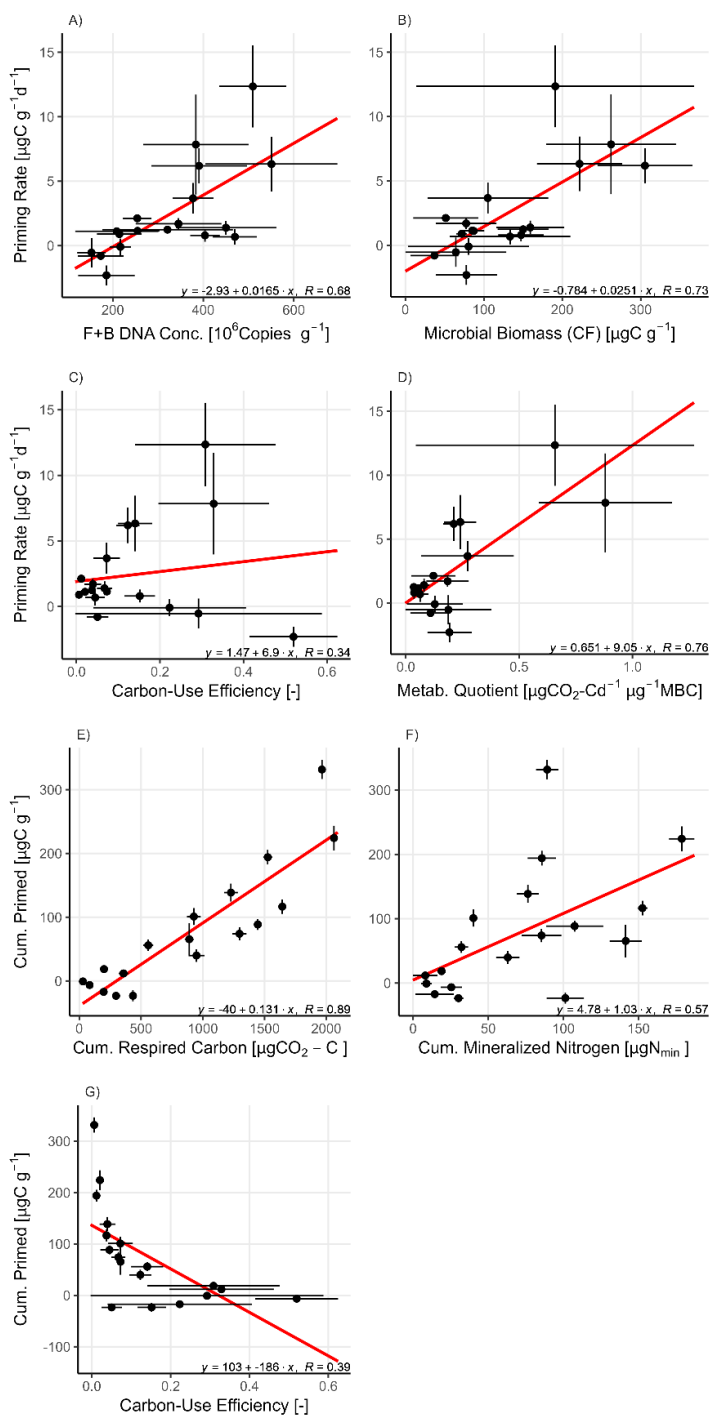


Figure 2.4 Regression plots for correlations of interest between priming effects and microbial response variables across different treatments and sampling days:

- A)** priming rate and total microbial DNA concentration
- B)** priming rate and microbial biomass carbon
- C)** priming rate and CUE
- D)** priming rate and $q\text{CO}_2$
- E)** cumulative priming and cumulative respired carbon
- F)** cumulative priming and cumulative mineralized nitrogen
- G)** cumulative priming and CUE. $n=3$ for each mean data point with standard error as error bars.

2.3.4 Relationships between organic amendment composition and microbial response variables

Relationships of OA composition with MRVs were strongest for $C_{DO}:C_{HW}$ which showed by far the highest number of significant correlations (37) with MRVs across all sampling days (Table 2.4). Significant correlations between MRVs and stoichiometric characterizations were fewer (≤ 28). Overall, the $C_{TOT}:N_{TOT}$ characterization showed more significant correlations across sampling days than other C:N characterizations. No stoichiometric characterizations demonstrated good correlation with peak changes in more than three MRVs. The highest number of correlations for MRV peak responses (8) were with N_I concentrations and most C_{DO} -related components (C_{DO} , $C_{DO}:C_{AH}$, $C_{DO}:C_{HW}$). The highest number of significant correlations (128) for all OA treatments and MRVs occurred on day 59.

Table 2.4 Number of significant correlations of OA composition with 11 MRVs, priming rates and cumulative priming. A higher number of significant correlations suggests a stronger relationship with the OA characterization. Underlined are those OA components that significantly correlated with the highest number of different MRVs and priming effects for a given sampling day.

Amendment Characterization		Day						Total	Peak Response	
		3	7	16	30	59	150			
Stoichiometric	C:N	C _{TOT} : N _{TOT}	2	7	3	2	7	6	<u>28</u>	3
		C _I :N _I	0	2	1	0	4	4	11	1
		C _{AH} :N _{AH}	1	8	0	0	4	3	16	1
		C _{HW} : N _{HW}	0	5	1	0	6	3	16	1
		C _{DO} : N _{DO}	0	3	0	1	4	4	12	1
N	N _{TOT}	4	8	4	3	4	3	26	7	
	N _I	7	6	6	6	4	3	<u>32</u>	<u>8</u>	
	N _{AH}	0	1	1	1	1	3	7	2	
	N _{HW}	3	4	3	4	10	6	31	5	
	N _{DO}	3	5	6	6	4	3	27	7	
Energetic	C	C _{TOT}	2	9	2	4	6	5	28	3
		C _I	2	9	3	4	6	5	29	4
		C _{AH}	2	10	3	3	6	6	<u>30</u>	3
		C _{HW}	2	2	2	2	10	6	25	3
		C _{DO}	3	5	6	5	5	4	28	<u>8</u>
C _x :C _{TOT}	C _I : C _{TOT}	3	6	3	4	8	6	<u>31</u>	6	
	C _{AH} : C _{TOT}	2	7	3	3	7	6	29	3	
	C _{HW} : C _{TOT}	2	3	2	2	8	6	23	3	
	C _{DO} : C _{TOT}	3	2	6	3	6	5	26	7	
C _{DO} :C _x	C _{DO} : C _I	3	2	6	3	6	6	27	7	
	C _{DO} : C _{AH}	3	2	7	3	8	6	30	<u>8</u>	
	C _{DO} : C _{HW}	7	9	7	5	4	5	<u>37</u>	<u>8</u>	
<i>Total correlations per day</i>		54	115	75	64	<u>128</u>	104	549	999	

2.3.5 Relationships between organic amendment composition and microbial peak response

The peak response of most MRVs demonstrates the strongest relationships for energetic characterizations where C_{DO} and $C_{DO}:C_{HW}$ showed the strongest linear correlation to most of the observed changes in MRVs (Figure 2.5, Appendix C). $C_{DO}:C_{HW}$ was the strongest significantly correlated OA characteristic for the peak response of microbial biomass by chloroform-fumigation extraction, total and bacterial DNA concentrations by ddPCR, and carbon and nitrogen mineralization rates. C_{DO} was the best-performing characterization for the peak response of fungal DNA concentrations, fungal to bacterial ratio (not significant), and N-mineralization rate (same strength as $C_{DO}:C_{HW}$). While qCO_2 showed a relatively stronger association with energetic OA components than stoichiometric ones, neither peak CUE nor qCO_2 demonstrated a statistically significant correlation with any of the investigated OA components (Appendix C). Overall, for all MRVs, carbon solubility fractions, and ratios among these fractions, tended to be better linear predictors than total C:N ratios.

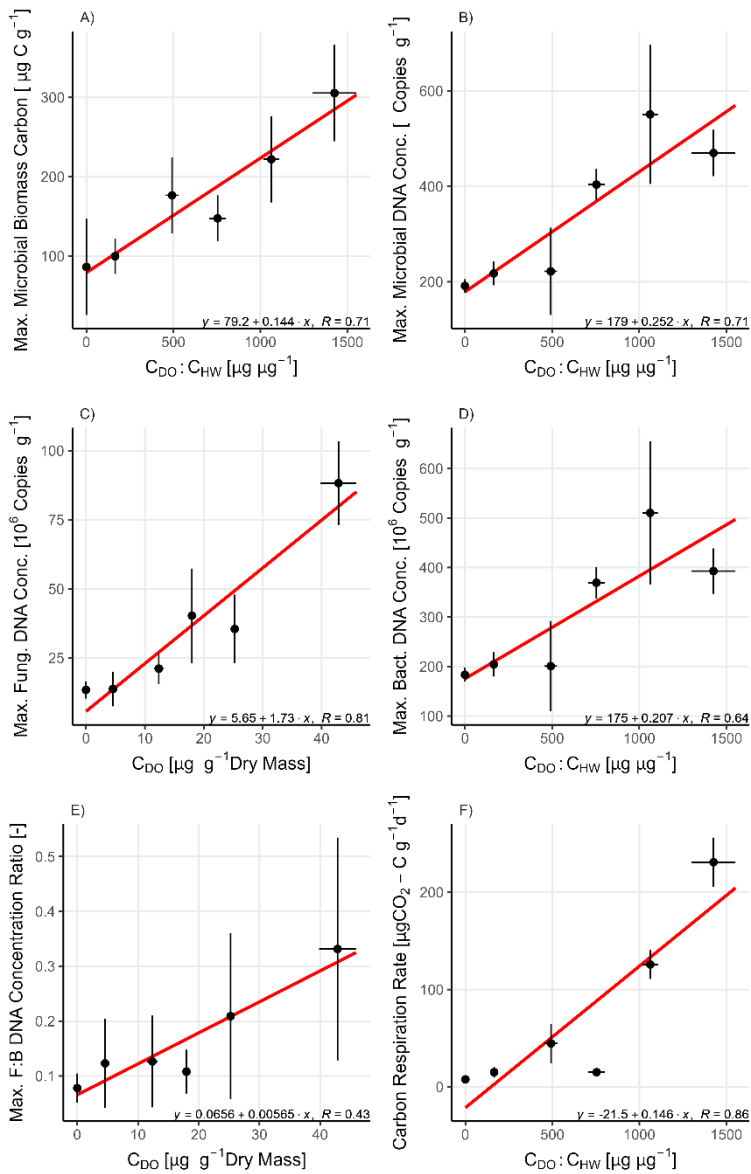


Figure 2.5 (continues on next page) Linear regression of peak response with highest correlative OA component for fungal abundance (A, B), bacterial abundance (C, D), and fungal to bacterial DNA ratio (E, F). Associated time-series data is presented in Appendix D, and table with correlation coefficients for all relationships is presented in Appendix C. n=3 for each mean data point with standard error as error bars.

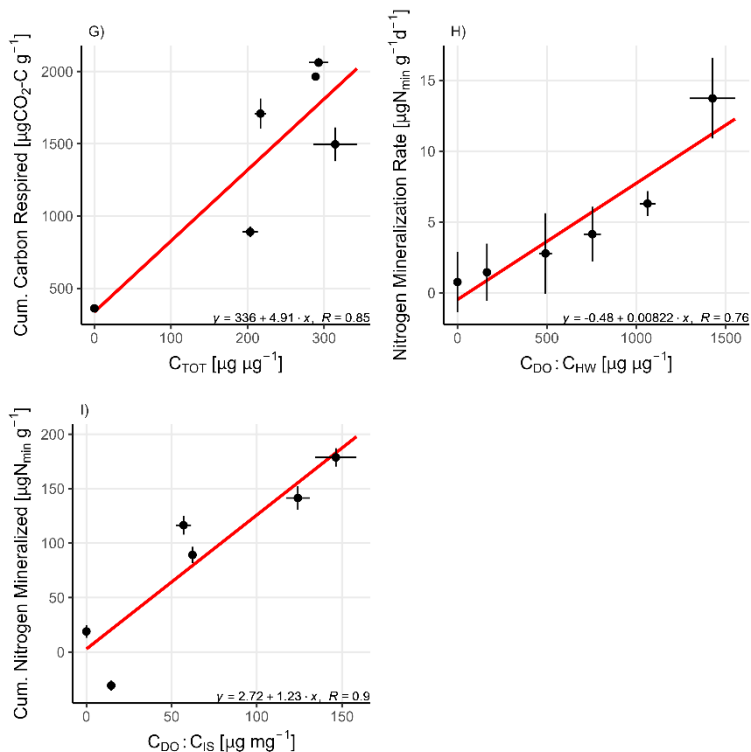


Figure 2.6 (continued) Linear regression of peak response with highest correlative OA component for fungal abundance (A, B), bacterial abundance (C, D), and fungal to bacterial DNA ratio (E, F). Associated time-series data is presented in Appendix D, and table with correlation coefficients for all relationships is presented in Appendix C. $n=3$ for each mean data point with standard error as error bars.

2.3.5 Relationships amongst microbial response variables

Many MRVs correlated with other MRVs (Appendix E). This is expected, as some calculated MRVs are directly derived from measured MRVs (these relationships are not further explored here). The strongest correlations per MRV ($R > 0.6$, $p < 0.001$) occurred between CUE and $q\text{CO}_2$ ($R = 0.65^{***}$), cumulative carbon and nitrogen mineralization ($R = 0.74^{***}$), and bacterial DNA concentrations and microbial biomass carbon by CF ($R = 0.7^{***}$). Also, a strong correlation between microbial biomass by CF and microbial DNA concentrations by ddPCR ($R = 0.72^{***}$) was observed, illustrating consistency between CF and ddPCR methods for determining microbial abundance. Most of these relationships can be considered linear or close to linear, although the relationship between the CUE and $q\text{CO}_2$ appears to be partly driven by two high values (Appendix F).

2.4 DISCUSSION

Interactions between priming effects, OA composition, and MRVs have been explored empirically and conceptually over the past decade. Yet, evidence for concepts describing these interactions are limited to those derived from investigations of which a scarce number apply natural OAs and that often involve only a few combinations of OA characterizations with priming effects and MRVs (Clocchiatti et al. 2020; Fang et al. 2020; Marzi et al. 2020; Stark et al. 2007; H. Wang et al. 2015). To address uncertainties arising from these caveats, we present an assessment of the relationships between the priming effect, multiple, differently characterized OAs, and several prominent MRVs, in order to integrally evaluate and compare i) the influence of organic amendment composition on priming effects (section 2.4.1), ii) the influence of changes in microbial response variables on priming effects (section 2.4.2), iii) the influence of organic amendment composition on changes in microbial response variables (section 2.4.3), and iv) the implications of applying organic amendments in agriculture for SOC sequestration (section 2.4.4).

2.4.1 Relationship of priming effects with organic amendment composition

Priming rate and cumulative priming correlated directly with most characterizations of OA composition. While relationships of priming effects with stoichiometric indexes have been observed in previous studies (Lijun Chen et al. 2019; Liu et al. 2020), we could not find a study that integrally related priming effects to different energetic/biochemical characterizations of natural OAs. Some studies, however, have investigated priming effects related to artificial substitutes or pure applications of natural biochemical components using, for example, carbon substrates in the form of glucose and lignocellulose (Aye et al. 2018), a combination of OAs with glucose (Shahbaz et al. 2018), additions of pure cellobiose and vanillic acid (Di Lonardo et al. 2017), or, alternatively, characterized OAs solely based on lignin content (Stewart et al. 2015). These studies demonstrate how glucose additions (theoretically pure C_{DO}) induce greater priming effect than lignocellulose (more alike to C_{IS}). In this study, however, C_{DO} concentrations of natural OAs were not related to priming, while other labile components (i.e. C_{HW}) resulted not lower, instead of higher, priming effects. Relationships of priming effects with C_{DO} and other high-energy OA components form the basis of the co-metabolism theory which describes how the addition of high-energy OAs provides microorganisms with the energy required for the synthesis of extracellular enzymes capable of degrading SOC, thereby enhancing SOM mineralization and resulting in an enhanced priming effect (Kuzyakov et al. 2000). Absence of relationships of the priming effect with C_{DO} -related components of OAs, and negative relationships of priming with other high energy OA components (i.e. C_{HW}), suggests that

co-metabolism was not a dominant driver of the priming effects observed for the natural OAs investigated in this study.

Strongest relationship with priming is observed for the $C_{HW}:C_{TOT}$ ratio (Table 2.2). Its negative relationship with priming suggests that differences in OA composition, through a relative increase in C_{HW} or decrease in C_{TOT} (i.e. higher $C_{HW}:C_{TOT}$), can result in the inhibition of SOC mineralization (i.e. reduced priming). Quantification of this relationship shows that peak priming rates switch from positive to negative at C_{HW} concentrations greater than $120 \mu\text{g mg}^{-1}$. Negative priming effects are explained through the theory of preferential substrate utilization, which describes how, especially in the early phases of OA decomposition, low or negative priming might occur as microbes preferentially decompose easily degradable compounds of fresh OA over the recalcitrant compounds typically defining SOM (H. Wang et al. 2015; Werth and Kuzyakov 2010). As such, negative priming is typically observed for ‘labile’ substances, such as glucose or sucrose (Kuzyakov 2010) or highly labile litter types (Potthast, Hamer, and Makeschin 2010; H. Wang et al. 2015). Observed relationships of priming effects with the $C_{HW}:C_{TOT}$ ratio suggests that, of the different OA components investigated, the $C_{HW}:C_{TOT}$ is the strongest indicator for the preferability of microorganisms to decompose an OA over SOC, and therefore strongest indicator for identifying OAs with potentially reduced priming effects.

Somewhat counterintuitive to the suggestions of preferential substrate utilization, we observe negative priming effects for compost (Figure 2.3), a substrate that is widely recognized as resistant and largely depleted of most of its labile organic fractions (Lhadi et al. 2006). While it is likely that the composted product in this study differs from traditional compost, as we did not monitor for composting phases and associated microbial successions, the final product could still be characterized as recalcitrant given its significantly lower decomposition rates (Appendix D) and higher insoluble carbon concentrations (

Table 2.1). Based on these observations, we would not expect its preferable decomposition and subsequently negative priming. This contradiction suggests that inadequately defined labels of ‘lability’ and ‘recalcitrance’ are insufficient to describe the relationship between OA properties and priming effects, given that even OAs that are resistant to decomposition can, by the theory of preferential substrate utilization, contain compounds that might be preferentially decomposed resulting in negative priming. It would be more comprehensible to define and describe relationships between OAs and priming effects based on situationally independent properties such as, for instance, an OA’s $C_{HW}:C_{TOT}$ ratio, which in this study demonstrates the strongest relationship with priming effects.

While nitrogen dynamics, and principles of stoichiometric homeostasis, are undebatably influential on priming (Chen et al. 2014; Cui et al. 2020; Fang et al. 2020; Liu et al. 2020;

Zhu et al. 2021), observed similarity in strength of the relationships between stoichiometric and energetic characterisations suggests that stoichiometric characterizations are potentially not as critically important for predicting priming effects as is currently understood. Stoichiometry is attributed a central role in the ‘nutrient-mining’ theory, which stipulates that mismatched stoichiometry of OAs with the microbial community enhances microbial decomposition of SOM in attempts to accommodate for the introduced nutrient imbalances (Cui et al. 2020; Fujita, Witte, and van Bodegom 2014). In this study, markedly different priming effects, however, were observed for OAs sharing similar C:N ratio’s (i.e. 11.4 ± 0.7 for grasses, 10.1 ± 0.2 for compost, and 13.3 ± 0.7 for fermented grasses;

Table 2.1). Naturally, multiple mechanisms influencing priming can operate simultaneously, i.e. co-existence of nutrient-mining as well as co-metabolism pathways, where the dominance of specific mechanisms is influenced by many factors related to resource availability and composition as well as microbial community properties (Blagodatskaya and Kuzyakov 2008; Chen et al. 2014). The currently observed similarity between stoichiometric and energetic characterizations, however, allow for the presumption that energetic characteristics might have similarly important role in driving priming effects as is currently understood for OA stoichiometry. Given that OAs with greater stoichiometric differences are also likely to vary more in their energetic characterizations (e.g. wood chips;

Table 2.1), energetic characterizations might prove a more accurate means to predicting short-term priming effects than stoichiometric differences. It would be interesting for future studies to further explore the relative importance of OA energetic components versus stoichiometry with other OAs as this would help elucidate the relative importance of the many factors influencing priming, thereby similarly contributing to identifying which OA properties are desirable for efficient SOC sequestration.

2.4.2 Relationship of priming effect with changes in microbial response variables

Priming effects directly correlated with a number of changes in several MRVs (Table 2.3). Similar correlations have been described in other studies where priming was found to be related to changes in microbial biomass (Blagodatskaya and Kuzyakov 2008; L.-J. Li et al. 2018; Xiao et al. 2015), and fungal abundances (Fontaine et al. 2011; Liu et al. 2018). Here, we additionally observed weak but significant negative correlations of priming rate with changes in CUE and a positive correlations of cumulative priming with qCO_2 . Both CUE and qCO_2 are indirectly, inversely related, as each is an indicator of the efficiency of a microbial community in assimilating decomposed organic matter into biomass. The correlations observed for CUE and qCO_2 suggest that greater priming is associated with reductions in community metabolic efficiency. These changes in metabolic efficiency

potentially hint at changes in community physiology such as shifts in either K- or r-strategists dominance (Chen et al. 2014). Alternatively, or simultaneously, a microbial community might simply change its enzyme production in reaction to the composition and availability of resources in its environment. For instance, the decomposition of SOM, whether by co-metabolism or nutrient-mining pathways, likely offers a lower return on enzyme investment due to the limited physical or chemical accessibility of microbially decomposable compounds. Changes in community efficiency are therefore more likely an emergent factor rather than an explanatory factor in its relationship with priming effects.

2.4.3 Relationship of microbial response variables with organic amendment composition

Peak and intermittent MRVs were closely related to the C_{DO} concentrations (Table 2.4). Significant correlations with C_{DO} and C_{HW} were expected, as they define the more labile fractions of OAs, and, by both energetic and stoichiometric theories, higher energy characterizations of OAs (low C:N, high C_{DO} , C_{HW} , N_{DO} , $C_{DO}:C_{TOT}$ or $C_{HW}:C_{TOT}$) typically exert a greater influence on short-term changes in MRVs due to their high chemical accessibility to microbes. However, results demonstrated limited ability of traditional and novel stoichiometric characterizations of OAs to predict the response of MRVs – as evidenced from the few and minor correlations of the bulk C:N ratio ($C_{TOT}:N_{TOT}$) or the labile C:N ratio's ($C_{DO}:N_{DO}$, $C_{HW}:N_{HW}$) with both the peak and intermittent response of MRVs (Table 2.4, Appendix E). In other studies also lignin, phenol, and tannin measurements of OAs demonstrated closer relationships to decomposition rates than traditional, bulk C:N ratio's (Paustian et al. 1997).

While C_{DO} proves to be a strong predictor of the microbial response to OAs, it becomes a stronger predictor when it is proportionated to C_{HW} as the $C_{DO}:C_{HW}$ ratio. This is particularly true for microbial biomass by both CF and ddPCR methods, bacterial (B)-DNA concentrations, and carbon respiration and nitrogen mineralization rates. Results thus show that the ratio of carbohydrates, proteins, phenols, and lignin monomers in C_{DO} versus C_{HW} – including C_{HW} 's additional lipids (Balaria and Johnson 2013; Landgraf, Leinweber, and Makeschin 2006) – is a better indicator of the bioavailability of OAs than the traditional labile characterization by the stoichiometric C:N ratio or proximate C_{DO} , N_{DO} , or $C_{DO}:C_{TOT}$ fractions. The microbial responses show that, when C_{HW} is relatively greater than C_{DO} , C_{HW} may induce an inhibitory effect on the microbial activity as it results in a lower peak response. Potentially, the lipids contained in the C_{HW} protect OA components from enzymatic degradation (of e.g. C_{DO}) through either physical or chemical protection mechanisms – although further investigation is needed to verify this.

Stoichiometric theory describes how microbes strive to maintain stoichiometric homeostasis, yet limited correlation of MRVs with stoichiometric characterizations reveal that direct application of stoichiometric theory for the prediction of microbial response appears not so straightforward. The relatively weaker correlations between MRVs to OA stoichiometry might be explained by the chemical complexity of OAs. Chemically complex amendments may support a broader range of metabolic pathways in the soil (Hernández and Hobbie 2010; Kallenbach and Grandy 2011; Meier and Bowman 2010). The range of potential decomposition pathways may trigger different simultaneously active processes and mechanisms that could potentially obscure the effects of stoichiometric imbalances. Partially due to these complexities, the usefulness of the bulk C:N ratio in predicting soil response has been the subject of discussion given its unreliability in different environments where sometimes it demonstrates significant correlations (Benbi and Khosa 2014; L.-J. Li et al. 2018; Sauvadet et al. 2017), while in other cases often not (Bonanomi et al. 2019; Kallenbach and Grandy 2011; Li et al. 2016; L.-J. Li et al. 2018; Marzi et al. 2020). As an alternative, studies have proposed that the C:N ratio of specific biochemical OA fractions may provide stronger predictors of soil response. Yet, in a study with glucose and nitrate as artificial proxies for labile-C and labile-N, Liu et al. (2020) observed little contribution of the labile C:N ratio to the response in priming in both organic and mineral soils. In the current study, natural, C:N ratios in different solubility fractions similarly showed little correlation to the response of the investigated MRVs (Table 4, 5). While some strong and significant correlations of the bulk and fractional C:N ratios with MRVs were found (e.g. carbon and nitrogen mineralization, and the priming effect), its value is debatable given stronger or equally strong correlations with other OA components – e.g. the total nitrogen content in the case of the cumulative nitrogen mineralization. The current study thus confirms a general lack of correlation of traditional bulk C:N ratios with the peak and intermittent response of many prominent MRVs and also demonstrates limited correlation of more recently proposed stoichiometric indices such as the C:N ratio in solubility fractions. The generally low predictive capacity of the C:N ratio, whether in bulk or fractions, suggests that additional or more complex mechanisms than those currently illuminated in the stoichiometric theory may steer the observed short-term impact of OAs on soil microbial community dynamics.

2.4.4 Implications of organic amendment application for climate-smart agriculture

The application of OAs to arable land can contribute to closing resource cycles and building sustainable, climate-smart agricultural systems. Yet, the adoption of OA application practices is hindered by uncertainties regarding, amongst others, impacts on microbial

communities and soil carbon balances. Here, we outline and discuss the implications of current findings for applying OAs to agriculture and their impacts on soil properties.

The composition of OAs considerably influences soil carbon dynamics and priming effects (this study; (Clocchiatti et al. 2020; Fang et al. 2020; Marzi et al. 2020; Stark et al. 2007); therefore, SOC sequestration efficiency might be enhanced by changing OA composition through composting or fermenting OAs prior to their application. Our short-term incubation results suggest that composting OAs likely offers higher potential for efficient SOC sequestration than applying untreated OAs, given the observed lower carbon mineralization of compost (Appendix D), its smaller priming effect (Figure 2.3) and higher microbial CUEs (Appendix D). These findings are corroborated by a recent study where composted OAs demonstrated a more favourable (i.e. lower) priming effect than when applying fresh OAs (Lerch et al. 2019). However, compost likely has more gradual effects beyond the current incubation time that could offset its more favourable short-term impacts (<150 days). Furthermore, in addition to its limited priming, compost resulted in substantial nitrogen mineralization, suggesting that this treatment may be effective for the dual purpose of carbon sequestration and nitrogen fertilization.

As a second treatment option, bokashi fermentation resulted in an enhanced short-term priming and thus likely offers little benefit in enhancing SOC sequestration (Figure 2.3). Overall, compared to the untreated grasses treatment, bokashi fermentation resulted in similar changes in MRVs, especially in terms of changes in the metabolic quotient, yield efficiency, and priming effect. These results are in line with previous findings, which showed that changes in soil properties after application of a bokashi fermented product are mostly driven by the carrier substrate (i.e. the grasses) rather than being an effect (or interactive effect) of the fermentation process or the bokashi microorganisms (Mayer et al. 2010). Except for its potential fungal suppressive properties, given its lower fungal DNA-concentrations compared to untreated grasses, it is likely not worth the additional material and labour costs to create bokashi-fermented OAs at an agro-industrial level.

While important interactions between OA composition, soil microbial communities and soil carbon dynamics have been identified in previous studies, we still lack quantified relationships relating OA characteristics to soil changes such that they can be utilized to estimate OA impacts. Here we have identified which characterizations of OA composition best describe these different effects and quantified their relationships such that they may be used in preliminary evaluations of OAs. Results show, for example, how the application of OAs with: i) high $C_{HW}:C_{TOT}$ ratios significantly inhibit priming (Figure 2.3); ii) high $C_{DO}:C_{IS}$ ratios releases substantial amounts of mineral nitrogen (Figure 2.5I); and iii) high $C_{DO}:C_{HW}$ ratios results in greatest microbial biomass growth (Figure 2.5A, B). Validation and refining quantifications of these relationships by future studies involving additional and yet more diverse OAs would improve the confidence with which the relationships can be applied and

thereby contribute to the informed utilization of OAs in agriculture. Furthermore, in addition to the potential agronomic use, these relationships may serve as a basis for implementing microbially mediated carbon dynamics in both conceptual and deterministic soil models allowing for improved prediction of OA effects. Alternatively, they may serve as starting point for the further experimental investigation of the nexus of interactions between differently composed OAs, the microbial community, and soil carbon dynamics.

While these results shed more light on OA impacts, it is yet uncertain whether and precisely how these short-term changes impact long-term soil carbon balances and whether these changes persist or even accumulate with repeated (yearly) OA application. Furthermore, the highly significant relationships between numerous short-term responses in MRVs and labile OA components beckons the question of whether similar relationships exist between the intermediate to long-term response of MRVs and more stable OA components. OA impacts have furthermore demonstrated variation depending on soil type, and thus it would also be interesting to evaluate how these relationships change in different application settings. Addressing these questions is important, as OAs are among the most feasible instruments by which we can organically condition soil chemistry. Only by further developing our understanding of microbial response to OAs at different temporal and spatial scales can we hope to optimally and purposefully apply OAs in such a way that sustainable SOC sequestration efforts are maximally efficient and effective.

2.5 CONCLUSION

This study provides an integrated, quantitative assessment of the interactions between priming effects, different characterizations of OA composition, and soil microbial properties. We show: A) a close relationship of priming effects with the $C_{HW}:C_{TOT}$ ratio of applied OAs, where higher $C_{HW}:C_{TOT}$ ratios reduce priming effects; B) substantially more correlations of OAs' $C_{DO}:C_{HW}$ ratio with investigated soil microbial properties and their peak response than with other OA characterizations; and C) various correlations of MRVs such as microbial biomass, fungal and bacterial DNA-concentrations, carbon-use efficiency and metabolic quotients with observed priming effects. Findings indicate the strongest predictability of soil and microbial response to OAs based on energetic characterizations of OA composition, thereby advocating the adoption of energetic dynamics to model and predict microbially-mediated soil carbon dynamics. Additionally, findings show how composting, but not fermenting, OAs prior to application can potentially improve SOC sequestration efficiency by reducing their priming effect. These findings shed light on the interactions and impacts of OAs on soil properties, thereby contributing to the development of efficient, sustainable, climate-smart agricultural systems.